

Photocatalytic activity of ZnO nanoparticles synthesized from zinc nitrate and botanical extracts of neem, chrysanthemum, Mexican marigold and shiitake mushroom

Juan R. López-López,^a  Armando Tejada-Ochoa,^b 
Maritza E. Cervantes-Gaxiola,^a  José M. Herrera-Ramírez^b  and
Perla F. Méndez-Herrera^{a*} 

Abstract

Background: Green synthesis emerges as a need to obtain functional materials, but this also involves following certain principles that imply methods and inputs that are friendlier to health and the environment. A wide variety of materials can be synthesized under these principles, one of them being ZnO, which can be used for environmental, electronic and biomedical applications to mention a few. In this work, ZnO nanoparticles (NPs) were synthesized using aqueous extracts of neem, chrysanthemum, Mexican marigold and shiitake mushroom and subsequently used to degrade methylene blue (MB) under solar light irradiation. The NPs were characterized by UV–visible spectroscopy, transmission electron microscopy, X-ray diffraction, Fourier transform infrared spectroscopy and thermogravimetric analysis to investigate the structural, optical and electronic properties of the NPs.

Results: The results indicate the formation of hemispherical NPs with aggregates in a size range of 5.38–28.37 nm. All the samples presented a hexagonal wurtzite crystalline structure. The best photocatalytic performance for MB degradation was shown by ZnO NPs obtained using Mexican marigold ($0.0873 \pm 0.008 \text{ min}^{-1}$) followed by those obtained using shiitake mushroom ($0.0602 \pm 0.002 \text{ min}^{-1}$), neem ($0.0365 \pm 0.02 \text{ min}^{-1}$) and chrysanthemum ($0.0357 \pm 0.01 \text{ min}^{-1}$).

Conclusions: Botanical aqueous extracts have the potential to be used in the synthesis of semiconductor materials, as they allow the modification of the size and band gap. Many of the phytochemicals present in the extracts help to improve the interaction between catalyst and pollutants, in this case MB, and therefore have a positive impact on the degradation of textile pollutants.

© 2022 Society of Chemical Industry (SCI).

Keywords: zinc oxide; green synthesis; nanoparticles; solar photocatalysis

INTRODUCTION

Organic dyes are widely used in the pharmaceutical, textile, food, paint, paper and plastic industries, to name a few. However, the dumping or accidental discharge of organic dye wastewater affects aquatic bodies by inhibiting solar radiation and reducing oxygen concentration, causing environmental and health problems.^{1,2} In particular, methylene blue (MB) is the most commonly used thiazine dye in the textile industry, and prolonged exposure to MB produces harmful effects such as cyanosis and skin or gastrointestinal irritation in living beings.³ Photocatalytic degradation of organic dyes with the assistance of semiconductors has gradually been established as an efficient process for removing these pollutants.⁴ However, the removal of dyes from industrial waters through a sustainable and practical approach has attracted the attention of many researchers. In this sense, environmental nanotechnology has acquired great importance for the elimination of dangerous chemical substances, including dyes, with a notable potential to promote viable and economical synthesis.⁵ Among metal oxide nanoparticles (NPs), zinc oxide (ZnO) NPs

are considered excellent candidates for photocatalytic degradation and environmental remediation,^{6,7} mainly due to their electrochemical stability, high electron mobility and large surface area,⁸ coupled with low cost and nontoxicity.

ZnO NPs have been synthesized using numerous approaches and techniques, such as sol–gel,⁹ precipitation,¹⁰ hydrothermal methods,^{11,12} spray pyrolysis,¹³ chemical vapor deposition¹⁴ and ultrasound¹⁵ and microwave-assisted techniques.¹⁶ On the other hand, the green synthesis of NPs using plant extracts, like leaves, roots, flowers and seeds, is a cost-effective and ecological process,

* Correspondence to: Perla F. Méndez-Herrera, Universidad Autónoma de Sinaloa, Facultad de Ciencias Químico Biológicas, Av. Las Américas S/N, Culiacán, Sinaloa, CP 80000, México, E-mail: pmendez@uas.edu.mx

^a Facultad de Ciencias Químico Biológicas, Universidad Autónoma de Sinaloa, Culiacán, Mexico

^b Centro de Investigación en Materiales Avanzados, Laboratorio Nacional de Nanotecnología, Chihuahua, Mexico

which eliminates the high energy consumption and hazardous chemicals required by conventional techniques.¹⁷ The presence of various phytochemicals and enzymes (organic acids, flavones and quinones) in such plant extracts aids in the reduction or oxidation of a precursor material to ZnO NPs.⁷ Furthermore, the large-scale production of NPs from plant extracts can be considered the best option. Parameters such as temperature, pH, precursor concentration, plant extract concentration and reaction time substantially affect the formation, stabilization, amount produced and yield rate of green-synthesized ZnO NPs.¹⁸ However, among these parameters, temperature, precursor concentration and the type of plant extract play a dominant role in the formation of NPs.⁸

In the literature, many research works have been reported addressing the green synthesis of ZnO NPs using various plant extracts.^{5,19–27} There are some reports of ZnO NPs synthesized using neem (*Azadirachta indica*) extract. For instance, Singh *et al.*²⁸ reported the synthesis of ZnO NPs using an extract of neem leaves and their biomedical application in the interaction with calf-thymus DNA. Sohail *et al.*²⁹ synthesized ZnO NPs using neem extract and evaluated their application as potential nanoantibiotics against drug-resistant microbes along with various biomedical applications. Besides, Acharya *et al.*³⁰ reported the synthesis of ZnO NPs using *A. indica* extracts and their subsequent application for the fabrication of an ethanol vapor sensor.

On the other hand, reports of using extracts from *Tagetes erecta*, *Chrysanthemum morifolium* and *Lentinula edodes* are scarce. In particular, Ilangovan *et al.*³¹ reported the synthesis of ZnO NPs using aqueous extracts of *T. erecta* flowers and their antioxidant, antimicrobial and cytotoxic activity in the HeLa cell line. In our previous work³² we reported the green synthesis of ZnO NPs using extracts from *A. indica*, *T. erecta*, *C. morifolium* and *L. edodes* with zinc acetate as a precursor, and the photocatalytic behavior under irradiation of sunlight in the degradation of the MB dye was evaluated.

Although the green synthesis of ZnO NPs and their use in the photocatalytic degradation of dyes have been widely documented,^{2,33–35} today there are few reports where ZnO NPs have been produced by green synthesis with extracts of *A. indica*, *T. erecta*, *C. morifolium* and *L. edodes* and used for the same purpose. Considering the wide availability of these four plants, ZnO NPs were synthesized in the investigation reported here using their extracts and zinc nitrate as the precursor. The NPs obtained were used to evaluate their photocatalytic activity in the degradation of MB dye and analyze the effect of the type of extract on the percentage of dye degradation.

MATERIALS AND METHODS

Reagents and materials

The experimental development was carried out with analytical-grade chemical reagents, which were used as acquired without further purification. Zinc nitrate (99%), sodium hydroxide (95%) and ethanol (96%) were supplied by FagaLab, ICR and Alfimex, respectively. Neem (*A. indica*) leaves were collected from trees planted in our Faculty of Chemical and Biological Sciences facilities. Chrysanthemum (*C. morifolium*) and Mexican marigold (*T. erecta*) flowers as well as shiitake mushrooms (*L. edodes*) were purchased from a local market. Prior to use, the botanical material was cleaned with distilled water, dried in a tray dryer and stored.

Preparation of aqueous extracts

Aqueous extracts were prepared as follows. For the neem extract, 50 g of ground neem leaves was added to 500 mL of distilled

water at 60 °C for 30 min, until the color of the water turned brown. Then, the obtained mixture was allowed to cool to room temperature and filtered. The chrysanthemum, Mexican marigold and shiitake mushroom extracts were obtained using the procedure described above, except that 25 g of ground material was used. The extracts obtained after filtration were stored at 4 °C for further experiments.

Synthesis of ZnO NPs

An amount of 100 mL of 0.5 mol L⁻¹ zinc nitrate solution was mixed with the same volume of each aqueous extract (*A. indica*, *C. morifolium*, *T. erecta* or *L. edodes*) in constant agitation, and then a 1 mol L⁻¹ NaOH solution was added dropwise until a pH of 7 was reached. The zinc nitrate–extract solution was heated at 70 °C for 1 h, then filtered and washed twice with distilled water and ethanol. Once filtered, the precipitate was dried at 80 °C overnight. Finally, the powder was sintered at 400 °C for 1 h.

Characterization of ZnO NPs

Absorption spectra (UV–visible) were obtained from ZnO NPs dispersed in water (0.01 g in 100 mL) and recorded in a wavelength range from 325 to 600 nm using a Velab spectrophotometer (VE-5100UV). Fourier transform infrared (FTIR) spectra were obtained in a range from 4000 to 440 cm⁻¹ using a System GX developed by PerkinElmer. A Hitachi 7700 transmission electron microscopy (TEM) instrument with an accelerating voltage of 100 kV was used to obtain selected area electron diffraction (SAED) patterns and to observe morphology. The Miller indices identification of SAED patterns was made with Crystallographic Tool Box (CrystBox) software using the ring analysis mode (ring graphical user interface). X-ray diffraction (XRD) patterns of ZnO nanostructures were recorded employing a Panalytical X'Pert3 MRD diffractometer using monochromatic Cu-K α radiation ($\lambda = 0.1542$ nm), the analysis being carried out in the 2θ range from 20° to 80° using a step size of 0.05°. The Scherrer method according to Eqn (1)³⁶ was used to determine the average crystallite size (D) of NPs:

$$D = \frac{0.9\lambda}{\beta \cos(\theta)} \quad (1)$$

where λ corresponds to the X-ray wavelength, β is the full width at half-maximum intensity and θ is the diffraction angle.

Finally, thermogravimetric analysis was performed with Q600 equipment developed by TA Instruments from ambient temperature up to 800 °C with a heating rate of 10 °C min⁻¹ in air atmosphere. The ZnO NPs were placed into an alumina pan with an initial weight of around 30 mg.

Evaluation of photocatalytic degradation

The photocatalytic behavior of the ZnO NPs was evaluated in the degradation of a dye, MB, by direct sunlight irradiation (689–765 W m⁻² in Culiacán, Sinaloa). This study was conducted according to the following procedure. First, 1 g L⁻¹ of each type of nanoparticulate material was placed in a reactor volume of 300 mL containing MB at a concentration of 10 mg L⁻¹ (C_0), adjusting the pH to 10, this value being selected according to previously reported pH optimization results.^{32,37} Then, the solution was placed in dark conditions with agitation for 45 min to achieve adsorption–desorption equilibrium. Subsequently, the solution was exposed to solar irradiation, taking samples every 15 min and centrifuging them at 12 000 rpm to eliminate nanoparticle interferences. Then samples were analyzed using UV–visible

spectroscopy in the range of 450–750 nm. Finally, the removal efficiency was calculated according to Eqn (2):

$$\text{Degradation (\%)} = \left(\frac{C_0 - C_x}{C_0} \right) \times 100 \quad (2)$$

where C_0 is the initial concentration and C_x is the concentration at time t .

RESULTS AND DISCUSSION

Characterization of ZnO NPs

UV-visible spectroscopy

The UV-visible spectroscopic analysis (Fig. 1(a)) shows the absorption band of ZnO NPs between 362 and 379 nm obtained in the presence of the different botanical extracts. However, the spectra of ZnO NPs synthesized in the presence of *C. morifolium* and *T. erecta* extracts show a red shift in the absorption edge. This may be due to the changes in their morphologies, particle size and surface microstructures. In the literature, it has been reported that ZnO particles that exhibit absorption at a higher wavelength in the UV-visible spectrum have a larger particle size. Additionally, due to the poor definition of the absorption bands, agglomeration of the particles can be inferred.

These results are in agreement with those reported in the literature for similar materials obtained via green chemistry.^{38,39}

From the UV-visible spectral data, Tauc plots were obtained to determine the band gap of the materials (Fig. 1(b)). The acquired band gap values were 2.76, 2.81, 3.00 and 2.72 eV for ZnO NPs obtained using *C. morifolium*, *T. erecta*, *L. edodes* and *A. indica*, respectively. The values are similar to those obtained for other ZnO NPs.^{40,41}

X-ray diffraction

The XRD patterns (Fig. 2) each exhibit 11 diffraction peaks, which confirm the hexagonal structure of crystalline ZnO NPs in accordance with the standard values reported in JCPDS no. 36-145.⁴² No additional peaks are observed, indicating that the synthesis

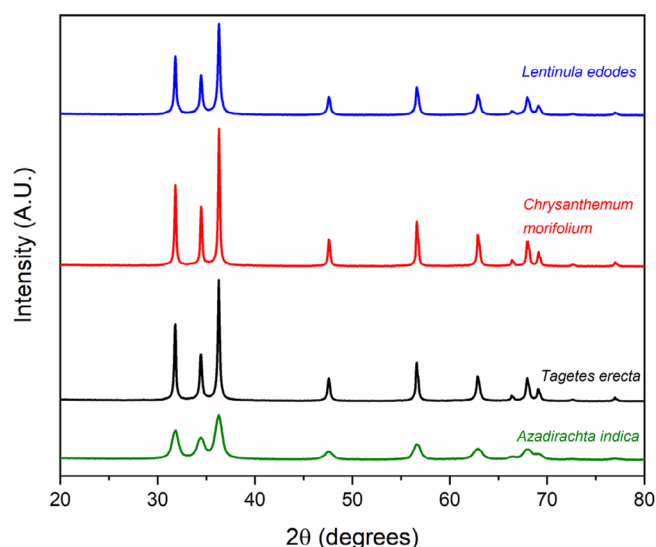


Figure 2. XRD patterns of ZnO NPs synthesized using the various botanical extracts.

procedure was performed correctly; therefore, no impurities are present.

Nevertheless, the type of extract used during the synthesis appears to have a significant influence on the intensity and broadening of the diffraction peaks, indicating that the crystallite size of the ZnO NPs can change as a result. The XRD pattern of the ZnO NPs synthesized with *A. indica* shows the lowest intensity and broadest peaks (Fig. 2). The XRD patterns of ZnO NPs synthesized with *C. morifolium* and *T. erecta* extracts present sharp and narrow peaks, indicating a greater crystallite size. Table 1 confirms the above findings based on Scherrer analysis.

It is important to highlight the effect of the botanical extracts on the crystallite size, since the various functional groups present in the extracts can help to control the size of the synthesized materials.

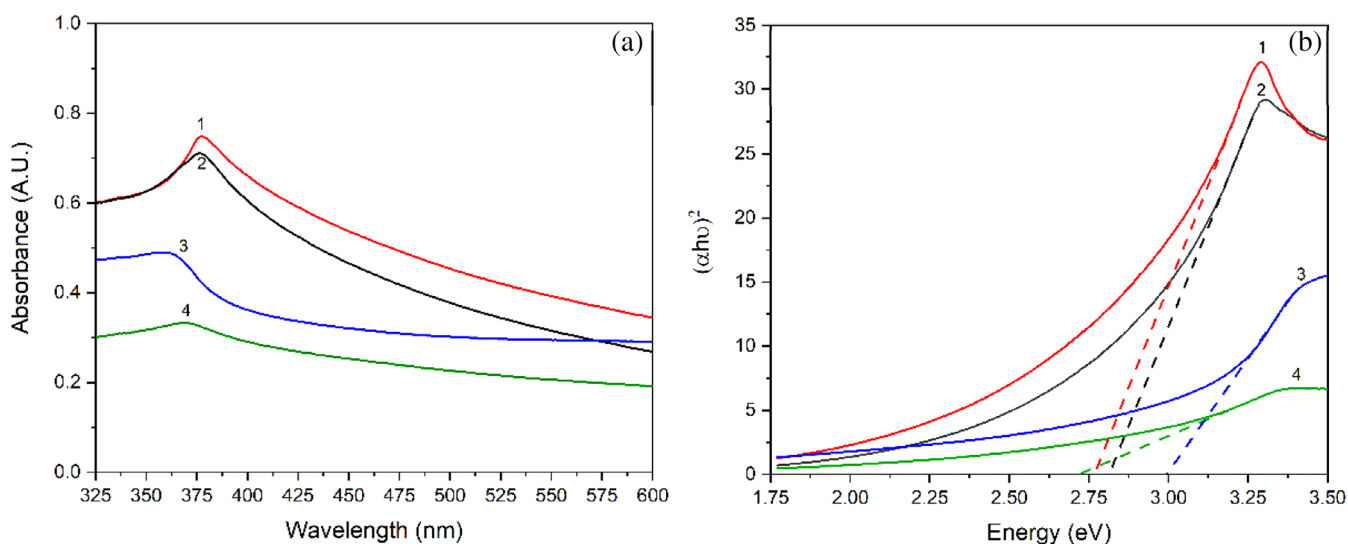


Figure 1. (a) UV-visible spectra and (b) Tauc plots of ZnO nanoparticles synthesized in the presence of: (1) *Chrysanthemum morifolium*, (2) *Tagetes erecta*, (3) *Lentinula edodes* and (4) *Azadirachta indica*.

Table 1. Crystallite size of ZnO NPs		
Extract	Crystallite size (nm)	SD ^a (nm)
<i>Azadirachta indica</i>	7.99	0.27
<i>Tagetes erecta</i>	28.96	3.74
<i>Chrysanthemum morifolium</i>	32.27	2.14
<i>Lentinula edodes</i>	26.27	2.02

^a Standard deviation.

Thermogravimetric analysis

Figure 3 displays the thermograms of all the synthesized materials, where an average mass loss of $2.696 \pm 0.76\%$ is observed. These results indicate that the nanostructures are stable since the observed mass loss is attributable to the release of absorbed water and loss of functional groups of the botanical extracts.

Transmission electron microscopy

The TEM images obtained for each nanomaterial are shown in Fig. 4. The NPs present a spherical and hemispherical morphology of various sizes (Table 2) depending on the extract used and, therefore, on the phytochemicals present in it, which are responsible for acting as capping agents. These results show that using *L. edodes* extract it is possible to synthesize smaller particles. In addition, using *T. erecta* and *L. edodes* extracts a narrower particle size variation was obtained. On the other hand, the SAED pattern (Fig. 4(e)) indexing indicates that the ZnO NPs present a hexagonal wurtzite structure; the presence of the Debye–Scherrer rings indicates that the selected zone is polycrystalline. Although the SAED pattern of only one sample is displayed, similar results were obtained for all the other samples. The results are in agreement with others obtained for the same type of NPs synthesized with different botanical extracts.^{43,44}

FTIR spectroscopy

Figure 5 shows FTIR spectra of ZnO NPs synthesized using the different plant extracts. All the spectra exhibit a band at 547 cm^{-1}

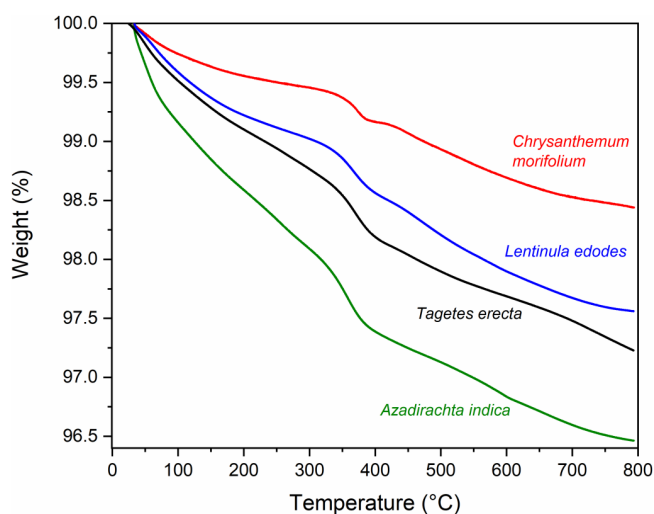


Figure 3. TGA curves of ZnO NPs synthesized using the various botanical extracts.

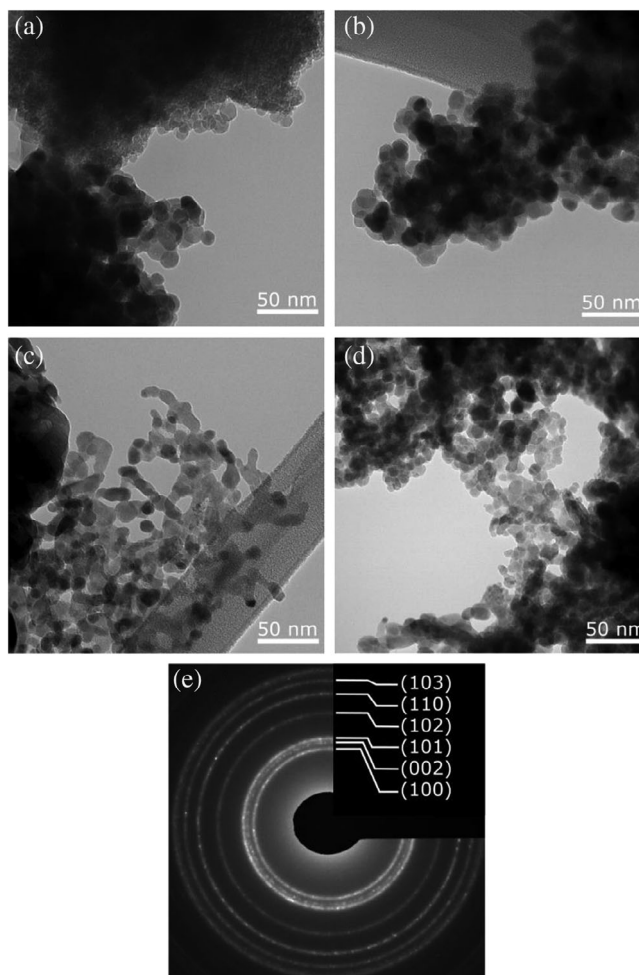


Figure 4. TEM images of ZnO NPs synthesized with: (a) *Azadirachta indica*, (b) *Tagetes erecta*, (c) *Chrysanthemum morifolium* and (d) *Lentinula edodes*. (e) Indexed SAED pattern taken from the ZnO NPs obtained with *Lentinula edodes*.

assigned to the presence of ZnO NPs,⁴⁵ which supports the formation of ZnO using different botanical extracts. Besides, the FTIR spectra of ZnO NPs show additional bands at 3408 , 1582 , 1426 , 1412 , 1119 , 1063 , 1020 and 870 cm^{-1} , which are due to the presence of various functional groups related to the byproducts resulting from the usage of *A. indica*, *T. erecta*, *C. morifolium* and *L. edodes* aqueous extracts. The vibrational stretching bands at 3408 and 1426 cm^{-1} represent O–H groups in ZnO NPs.⁴⁶ The less prominent absorption band at 1582 cm^{-1} is indicative of C–C stretching (in ring) of aromatics and N–H bending of primary amines.^{46,47} The band at 1412 cm^{-1} is assigned to C–C stretching.⁴⁸ The band at 1119 cm^{-1} corresponds to C–O stretching vibrations of carboxylic acids, alcohols, esters and ethers.⁴⁹ The band at 1063 cm^{-1} may correspond to the C–O stretch of alcohols, carboxylic acids, esters and ethers, and C–N stretching of aliphatic amines. The band at 1020 cm^{-1} is assigned to the stretching of two O–C bonds.⁵⁰ Finally, the band at 870 cm^{-1} is indicative of C–H bending of aromatic compounds.⁵¹ It is important to mention that most of the bands are stronger in the spectra of ZnO NPs synthesized using *T. erecta* and *L. edodes* extracts. The active biocompounds from the botanical extracts could be responsible for the reduction and

Table 2. Size variation of ZnO NPs

Extract	Particle size variation (nm)	Average (nm)	SD ^a (nm)
ZnO– <i>Azadirachta indica</i>	9.46–19.53	13.98	3.01
ZnO– <i>Tagetes erecta</i>	14.19–20.26	16.67	2.21
ZnO– <i>Chrysanthemum morifolium</i>	9.83–28.37	15.59	5.71
ZnO– <i>Lentinula edodes</i>	5.38–13.19	9.84	2.19

^a Standard deviation corresponds to the measurement of 30 samples.

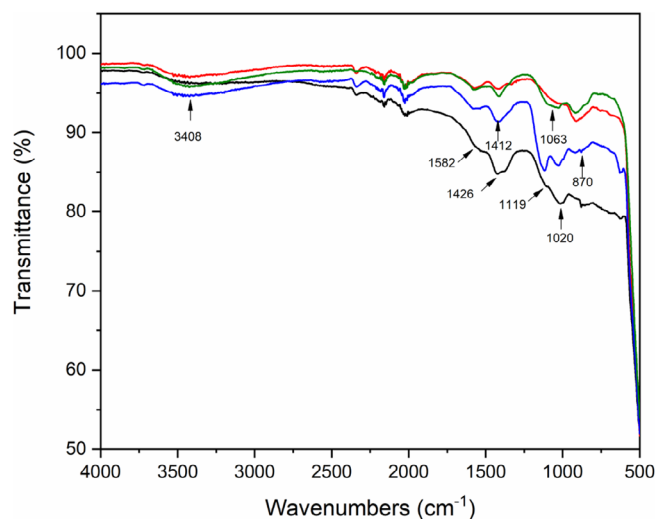


Figure 5. FTIR spectra of ZnO NPs synthesized with: (—) *Tagetes erecta*, (—) *Azadirachta indica*, (—) *Chrysanthemum morifolium* and (—) *Lentinula edodes*.

stabilization of the NPs (phenolic compounds, carboxylic acids, amines, etc.).

Photocatalytic activity

Dyes are used in various types of industries, so they are commonly prevalent in wastewater, and therefore some bodies of water may be affected. Their presence represents a risk for a variety of aquatic organisms but also for people. Due to their impact, the treatment of these types of pollutants is being addressed by researchers worldwide. In this sense, one of the most used materials for the treatment of dyes is ZnO, which has reported high efficiencies in the photodegradation of several dyes such as MB,⁵² rhodamine B,⁵³ methyl orange⁵⁴ and Congo red,⁵⁵ to mention a few. Figure 6(a) shows the UV–visible absorption spectra of the photocatalytic degradation of MB in the presence of ZnO NPs synthesized with Mexican marigold extract, while Fig. 6(b) presents the change in dye concentration for all extracts used. It is possible to note that the complete photodegradation of MB in sunlight occurred within 60 min in the presence of ZnO NPs synthesized using *T. erecta* extract.

Depending on the extract used during the synthesis, the properties of ZnO NPs can be different which is attributed to the presence of different phytochemicals in each botanical material used. Even if the sizes of ZnO NPs are quite similar, the remaining presence of phytochemicals after thermal treatment, in some cases, benefits the degradation of the dye, such as in the case of

best-performing systems involving *T. erecta* and *L. edodes* extracts. It has been reported that Mexican marigold has a high concentration of antioxidants, phenolics and flavonoids, such as rutin, quercetin, myricetin and lucenin.⁵⁶ On the other hand, *L. edodes* may contain proteins and vitamins (C, B3, B6 and D), as well as phenolic compounds and flavonoids (catechin and quercetin).⁵⁷

With the information obtained from Fig. 6(b), graphs of $\ln(C_0/C_x)$ were constructed, and the kinetic constant was determined (Fig. 7). This constant is considered according to a pseudo-first-order kinetic reaction according to the following equation⁵⁸:

$$\ln\left(\frac{C_0}{C_x}\right) = k_{app}t \quad (3)$$

where C_0 is the initial MB concentration (10 mg L⁻¹), C_x is the residual dye concentration in solution after a certain time, k_{app} is the rate constant (min⁻¹) and t is the exposure time to sunlight (min).

Table 3 exhibits a compilation of the calculated k_{app} values, which consider the processes of adsorption, photolysis and photocatalysis determined from Fig. 7. Table 3 also compares our results with those of other research groups that used green chemistry.

The apparent rate constant (k_{app}) is affected by the type of botanical extract used as follows: *C. morifolium* < *A. indica* < *L. edodes* < *T. erecta*. The difference lies in the composition of the phytochemical profile present in the extracts and in those that may remain anchored in the NPs even after heat treatment. Similar behavior was observed in other research, which highlights the importance of the phytochemicals in the extracts and their effect on the formation and stabilization of the NPs and their photocatalytic properties.^{65,66}

Comparing our results with those of other research groups reveals that the rate constants are within the order reported in the literature and, in some cases, with better performance in terms of photocatalytic rate. This difference in the photocatalytic rate is associated with the type of phytochemicals present in the extract, which can modify the band gap and size of the NPs and thus influence the performance of the material.

Mechanism of photocatalytic degradation of MB

MB in aqueous medium shows two characteristic peaks of monomers at 665 nm and dimers at 615 nm (Fig. 6(a)).⁶⁷ At the end of 45 min in the dark, a significant decrease in the absorption of both peaks is observed without modification in the wavelength, which is due to the adsorption capacity of the material. Once the samples begin to be irradiated with sunlight, an even greater

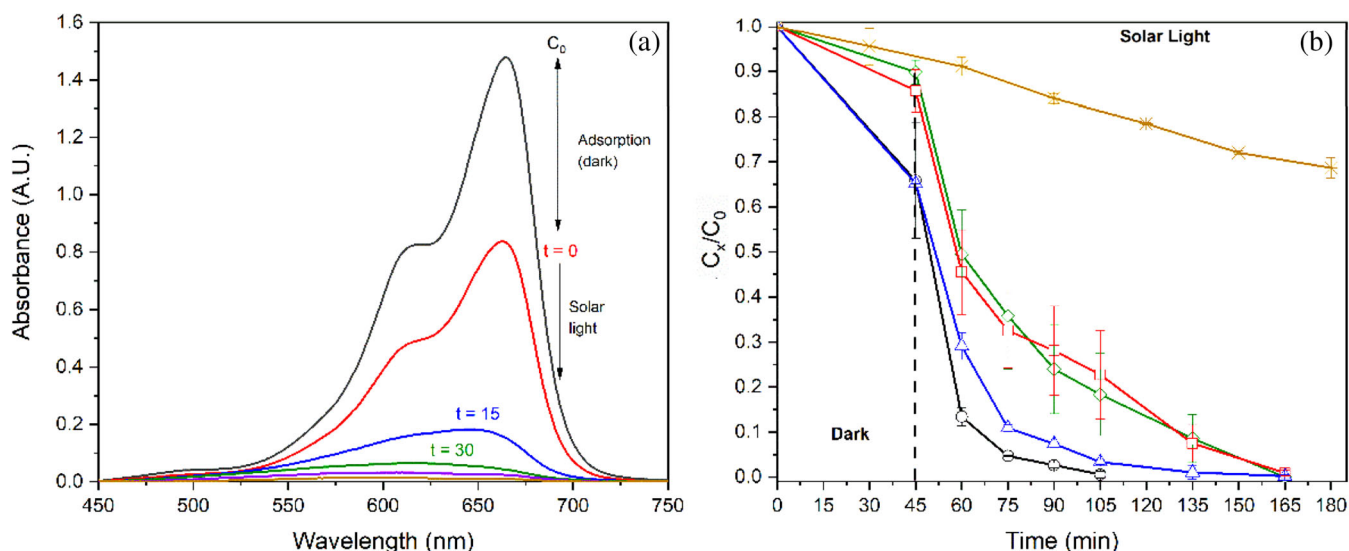


Figure 6. (a) Absorption spectra of MB with ZnO–*Tagetes erecta* NPs. (b) C_x/C_0 plots of MB with (—) photolysis, (—) *Tagetes erecta*, (—) *Azadirachta indica*, (—) *Chrysanthemum morifolium* and (—) *Lentinula edodes*. The first 45 min correspond to MB adsorption–desorption during dark equilibrium.

Table 3. MB dye photocatalyst performance under UV and sunlight irradiation over various green-synthesized ZnO NPs

Extract	Crystal size (nm)	Irradiation source	[MB]	Degradation (%)	Time (min)	Rate constant (min^{-1})	Ref.
<i>Scutellaria baicalensis</i>	~50	UV lamp	50 $\mu\text{mol L}^{-1}$	98.6	210	0.016	59
<i>Codonopsis lanceolata</i>	—	UV lamp	50 mmol L^{-1}	90.3	40	0.057	60
<i>Syzygium cumini</i>	11.35	Sunlight	40 mg L^{-1}	91.4	180	0.005	61
Fresh cow dung	~10	UV lamp	5 mg L^{-1}	99.9	100	0.05675	62
<i>Echinops kebericho</i>	14.67–19.66	Sunlight	10 mg L^{-1}	92.2	120	0.015	63
<i>Rosmarinus officinalis</i>	14.7–15.5	Sunlight	10 mg L^{-1}	99.64	45	—	64
<i>Azadirachta indica</i>	9.46–19.53	Sunlight	10 mg L^{-1}	100	120	0.0365 ± 0.02	This work
<i>Tagetes erecta</i>	14.19–20.26	Sunlight	10 mg L^{-1}	100	60	0.0873 ± 0.008	This work
<i>Chrysanthemum morifolium</i>	9.83–28.37	Sunlight	10 mg L^{-1}	100	120	0.0358 ± 0.01	This work
<i>Lentinula edodes</i>	5.38–13.19	Sunlight	10 mg L^{-1}	100	120	0.0602 ± 0.002	This work

decrease is observed with a blue shift due to the hypsochromic effect.⁶⁸ It is also observed that the degradation rate of monomers is higher than that of dimers. When the reaction time is long enough (60 min for Mexican marigold extract), both monomers and dimers were completely decomposed. A proposed mechanism for the degradation of MB catalyzed by ZnO NPs under sunlight irradiance is presented in Fig. 8.

Once the catalyst is exposed to sunlight, the incident photons promote the separation of charge carriers, and electrons (e^-) acquire sufficient energy to jump from the valence band (VB) to the conduction band (CB) leaving holes (h^+) in their place.⁶⁹ The electrons in the CB interact with the oxygen (O_2) adsorbed on the ZnO NPs and superoxide radicals are generated ($\text{O}_2^{\cdot-}$). Moreover, the resulting protonation will give rise to HO_2^{\cdot} , which can combine with trapped electrons to generate H_2O_2 , which ultimately produces hydroxyl radicals (OH^{\cdot}) on the surface of the catalyst.^{69,70} While holes (h^+) in the VB act as an oxidizing agent that interacts with water producing highly reactive OH^{\cdot} radicals. These radicals come into contact with the adsorbed MB molecules and the photocatalytic

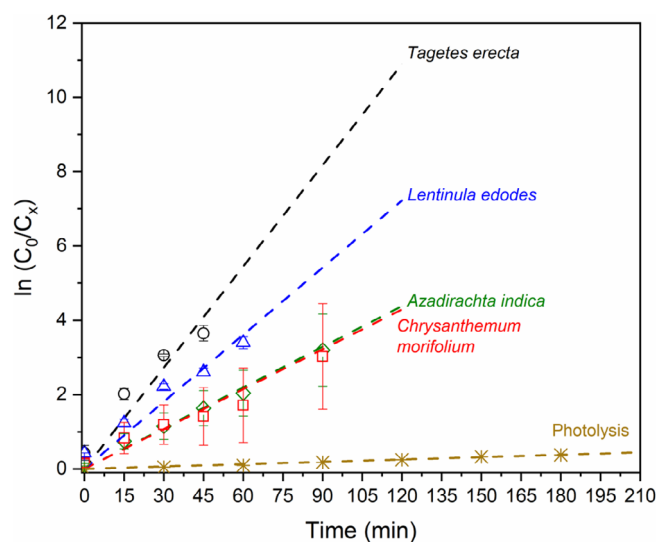


Figure 7. Plots of $\ln(C_0/C_x)$ as a function of sunlight exposure time of MB with the various catalysts.

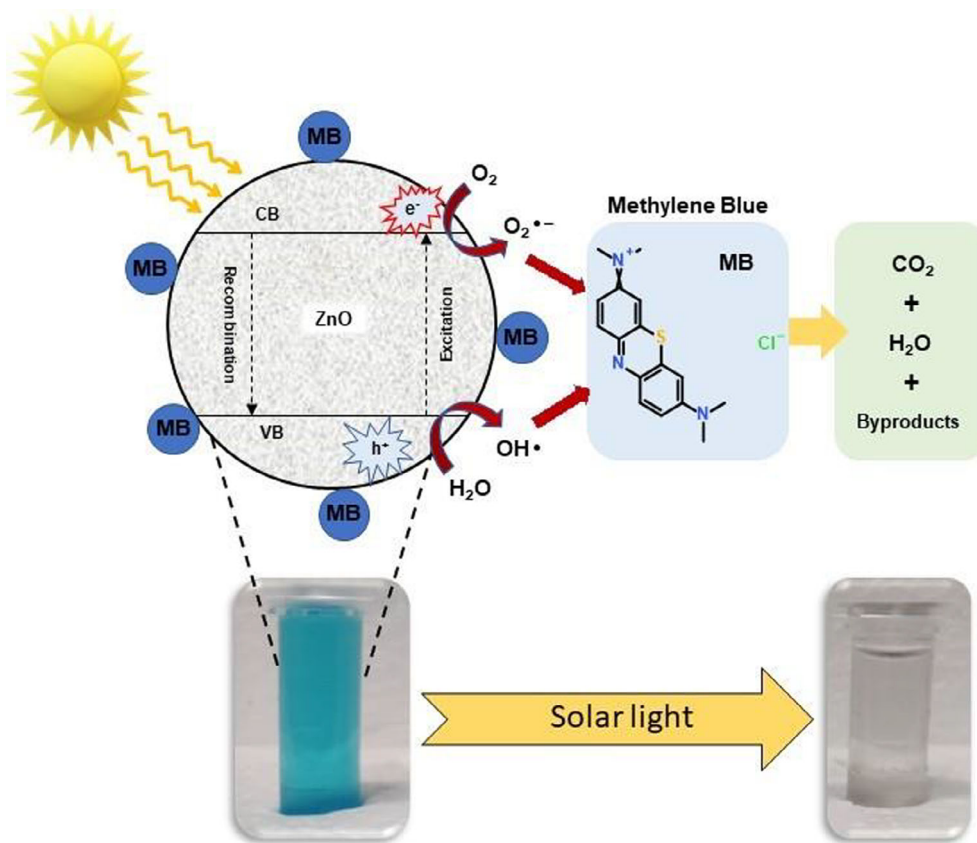
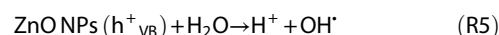
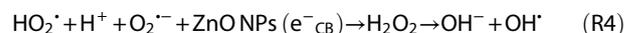
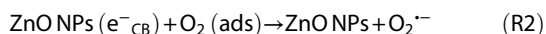
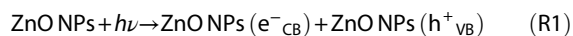


Figure 8. Proposed mechanism for photocatalysis process in the presence of organic pollutant MB on green-synthesized ZnO NPs. CB, conduction band; VB, valence band.

process proceeds with the oxidation of the dye.⁶⁹ These reactions can be shown as follows:



The oxidation products can be leucomethylene blue,⁷¹ single-ring structures or fully degraded to CO₂, Cl⁻, SO₄²⁻, NO₃ and H₂O.⁷² In further work, total organic carbon and high-performance liquid chromatography experiments will be carried out in order to know with certainty the degradation products and to establish an appropriate mechanism.

Recyclability of photocatalyst NPs

The NPs that showed the best photocatalytic performance (those synthesized using *T. erecta* extract) were used to test their stability and recyclability. They were first recovered by centrifugation and, once the supernatant was eliminated, they underwent a drying process in an oven at 100 °C for 2 h. The results of three reuse cycles are shown in Fig. 9. According to the results obtained, a slight decrease in the percentage of degradation can be seen with each cycle, with a maximum loss of 2.77% in the last cycle. This result indicates that the synthesized NPs are very stable and can be reused for several cycles, still with a good photocatalytic activity.

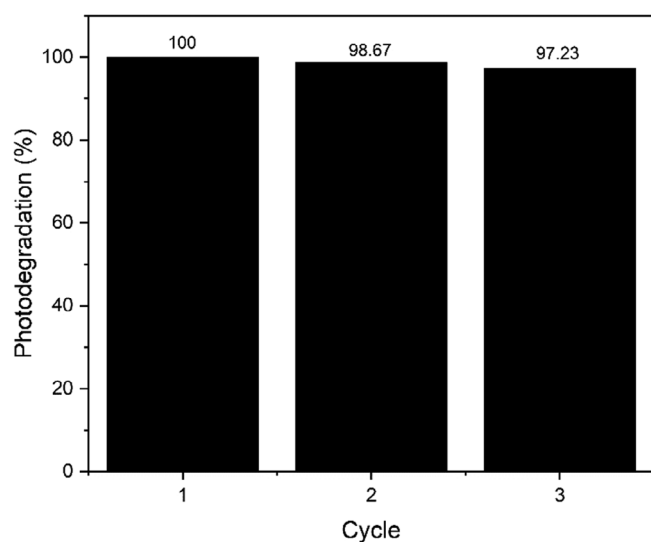


Figure 9. Recycling and reuse of ZnO NPs obtained in the presence of *Tagetes erecta*.

CONCLUSIONS

Green chemistry has brought several advantages to the synthesis of various materials, including semiconductors. Botanical extracts

influence the formation (size control) and stabilization of materials in different ways. The presence of some phytochemicals also favors the photocatalytic activity of the nanostructures, clear examples of which are antioxidants, flavonoids and phenolic groups, so different botanical specimens rich in these compounds should be sought. Extracts of Mexican marigold (*T. erecta*) and shiitake mushroom (*L. edodes*) improve the photocatalytic performance of NPs in the degradation of MB dye, degrading it entirely in 60 and 120 min, respectively. The synthesis method used is simple and environmentally friendly, and allows the successful use of the materials to treat a dye of pharmaceutical and industrial interest. Further studies of these NPs against other dyes and organic components will provide additional information on their performance and the possible correlation between the phytochemicals of the extracts and the pollutants to be treated.

ACKNOWLEDGEMENTS

The authors thank the program for promoting and supporting research projects of Universidad Autónoma de Sinaloa (PRO-A8-002 and PRO-A8-003). The authors also thank RA Ochoa-Gamboa, CE Ornelas-Gutiérrez, D Lardizabal-Gutiérrez and M Román-Aguirre for their technical support.

CONFLICT OF INTEREST

The authors declare no financial or commercial conflict of interest.

REFERENCES

- Chan S, Wu T, Juan JC and Teh C, Recent developments of metal oxide semiconductors as photocatalysts in advanced oxidation processes (AOPs) for treatment of dye wastewater. *J Chem Technol Biotechnol* **86**:1130–1158 (2011).
- Khan M, Ware P and Shimpi N, Synthesis of ZnO nanoparticles using peels of *Passiflora foetida* and study of its activity as an efficient catalyst for the degradation of hazardous organic dye. *SN Appl Sci* **3**:528 (2021).
- Hamdaoui O and Chiha M, Removal of methylene blue from aqueous solutions by wheat bran. *Acta Chim Slov* **54**:407–418 (2007).
- Odoom-Wubah T, Osei W, Chen X, Sun D, Huang J and Li Q, Synthesis of ZnO micro-flowers assisted by plant-mediated strategy. *J Chem Technol Biotechnol* **91**:1493–1504 (2015). <https://doi.org/10.1002/jctb.4748>.
- Narath S, Koroth SK, Shankar SS, George B, Mutta V, Waclawek S *et al.*, Cinnamomum tamala leaf extract stabilized zinc oxide nanoparticles: a promising photocatalyst for methylene blue degradation. *Nanomaterials* **11**:1558 (2021). <https://doi.org/10.3390/nano11061558>.
- Singh J, Dutta T, Kim K-H, Rawat M, Samddar P and Kumar P, 'Green' synthesis of metals and their oxide nanoparticles: applications for environmental remediation. *J Nanobiotechnology* **16**:84 (2018).
- Singh J, Kumar S, Alok A, Upadhyay SK, Rawat M, Tsang DCW *et al.*, The potential of green synthesized zinc oxide nanoparticles as nutrient source for plant growth. *J Clean Prod* **214**:1061–1070 (2019).
- Fagier MA, Plant-mediated biosynthesis and photocatalysis activities of zinc oxide nanoparticles: a prospect towards dyes mineralization. *J Nanobiotechnology* **2021**:6629180 (2021).
- Lee J, Easteal AJ, Pal U and Bhattacharyya D, Evolution of ZnO nanostructures in sol-gel synthesis. *Curr Appl Phys* **9**:792–796 (2009).
- Herrera-Rivera R, Olvera MDLL and Maldonado A, Synthesis of ZnO nanoparticles by the homogeneous precipitation method: use of Taguchi's method for analyzing the effect of different variables. *J Nanomater* **2017**:4595384 (2017).
- Wang Y and Li M, Hydrothermal synthesis of single-crystalline hexagonal prism ZnO nanorods. *Mater Lett* **60**:266–269 (2006).
- Mohan S, Vellakkat M, Aravind A and Reka U, Hydrothermal synthesis and characterization of zinc oxide nanoparticles of various shapes under different reaction conditions. *Nano Express* **1**:30028 (2020).
- Messing G, Zhang S-C and Jayanthi G, Ceramic powder synthesis by spray pyrolysis. *J Am Ceram Soc* **76**:2707–2726 (2005).
- Chen Z, Shum K, Salagaj T, Zhang W and Strobl K, ZnO thin films synthesized by chemical vapor deposition, in *2010 IEEE Long Island Systems, Applications and Technology Conference*, Vol. 10. IEEE, New York, pp. 1–6 (2010).
- Qian D, Jiang JZ and Hansen P, Preparation of ZnO nanocrystals via ultrasonic irradiation. *Chem Commun (Camb)* **34**:1078–1079 (2003).
- Thamima M and Karuppuchamy S, Microwave-assisted synthesis of zinc oxide nanoparticles. *Procedia Mater Sci* **11**:320–325 (2015).
- Sorbiun M, Shayegan Mehr E, Ramazani A and Mashhadi MA, Biosynthesis of metallic nanoparticles using plant extracts and evaluation of their antibacterial properties. *Nanochem Res* **3**:1–16 (2018).
- Singh A, Gautam PK, Verma A, Singh V, Shivapriya PM, Shivalkar S *et al.*, Green synthesis of metallic nanoparticles as effective alternatives to treat antibiotics resistant bacterial infections: a review. *Biotechnol Rep* **25**:e00427 (2020).
- El Shafey AM, Green synthesis of metal and metal oxide nanoparticles from plant leaf extracts and their applications: a review. *Green Process Synth* **9**:304–339 (2020).
- Bala N, Saha S, Chakraborty M, Maiti M, Das S, Basu R *et al.*, Green synthesis of zinc oxide nanoparticles using *Hibiscus subdariffa* leaf extract: effect of temperature on synthesis; anti-bacterial activity and anti-diabetic activity. *RSC Adv* **5**:4993–5003 (2015).
- Goutam S, Yadav A and Das AJ, Coriander extract mediated green synthesis of zinc oxide nanoparticles and their structural, optical and antibacterial properties. *J Nanosci Nanotechnol* **3**:249–252 (2017).
- Jayachandran A, Aswathy TR and Nair AS, Green synthesis and characterization of zinc oxide nanoparticles using *Cayratia pedata* leaf extract. *Biochem Biophys Rep* **26**:100995 (2021).
- Barzinjy AA and Azeez HH, Green synthesis and characterization of zinc oxide nanoparticles using *Eucalyptus globulus* Labill. leaf extract and zinc nitrate hexahydrate salt. *SN Appl Sci* **2**:991 (2020).
- Abel S, Tesfaye JL, Shanmugam R, Dwarampudi LP, Lamessa G, Nagaprasad N *et al.*, Green synthesis and characterizations of zinc oxide (ZnO) nanoparticles using aqueous leaf extracts of coffee (*Coffea arabica*) and its application in environmental toxicity reduction. *J Nanomater* **2021**:3413350 (2021).
- Handani S, Dahlan D, Arief S and Emriadi E, Green synthesis and characterization of zinc oxide (ZnO) nanoparticles using *Uncaria gambir* leaf extract, in Jakarta, ID, ed. *Empowering Science and Mathematics for Global Competitiveness*, Proc. SMIC 2018. CRC Press, London, pp. 3–8 (2019).
- Prachi K, Mushtaq A and Negi D, Green synthesis; characterization and antibacterial activity of zinc oxide nanoparticles using leaf extract of *Rubia cordifolia*. *Asian J Chem* **31**:385–388 (2019).
- Tănase MA, Marinescu M, Oancea P, Răducan A, Mihaescu CI, Alexandrescu E *et al.*, Antibacterial and photocatalytic properties of ZnO nanoparticles obtained from chemical versus *Saponaria officinalis* extract-mediated synthesis. *Molecules* **26**:2072 (2021). <https://doi.org/10.3390/molecules26072072>.
- Singh A, Neelam Y and Kaushik M, Physicochemical investigations of zinc oxide nanoparticles synthesized from *Azadirachta indica* (neem) leaf extract and their interaction with calf-thymus DNA. *Results Phys* **13**:102168 (2019).
- Sohail MF, Rehman M, Hussain SZ, Huma Z-E, Shahnaz G, Qureshi O *et al.*, Green synthesis of zinc oxide nanoparticles by neem extract as multifacet therapeutic agents. *J Drug Deliv Sci Technol* **59**:101911 (2020).
- Acharya TR, Lamichhane P, Wahab R, Chaudhary DK, Shrestha B, Joshi LP *et al.*, Study on the synthesis of ZnO nanoparticles using *Azadirachta indica* extracts for the fabrication of a gas sensor. *Molecules* **26**:7685 (2021). <https://doi.org/10.3390/molecules26247685>.
- Ilangoan A, Venkatramanan A, Thangarajan P, Saravanan A, Rajendran S and Kaveri K, Green synthesis of zinc oxide nanoparticles (ZnO NPs) using aqueous extract of *Tagetes erecta* flower and evaluation of its antioxidant; antimicrobial; and cytotoxic activities on HeLa cell line. *Curr Biotechnol* **10**:61–76 (2021).
- López-López J, Tejeda-Ochoa A, López-Beltrán A, Herrera-Ramírez J and Méndez-Herrera P, Sunlight photocatalytic performance of ZnO nanoparticles synthesized by green chemistry using different botanical extracts and zinc acetate as a precursor. *Molecules* **27**:6 (2022). <https://doi.org/10.3390/molecules27010006>.
- Davar F, Majedi A and Mirzaei A, Green synthesis of ZnO nanoparticles and its application in the degradation of some dyes. *J Am Ceram Soc* **98**:1739–1746 (2015).
- Singh K, Singh J and Rawat M, Green synthesis of zinc oxide nanoparticles using *Punica granatum* leaf extract and its application towards photocatalytic degradation of Coomassie brilliant blue R-250 dye. *SN Appl Sci* **1**:624 (2019).

- 35 Sukri S, Dayana E and Shamel K, Photocatalytic degradation of malachite green dye by plant-mediated biosynthesized zinc oxide nanoparticles. *IOP Conf Ser Mater Sci Eng* **808**:12034 (2020).
- 36 Jagodzinski HHP, Klug HP and Alexander LE, *X-ray Diffraction Procedures for Polycrystalline and Amorphous Materials*, 2nd edn. John Wiley & Sons, New York (1975).
- 37 Weldekirstos HD, Habtewold B and Kabtamu DM, Surfactant-assisted synthesis of NiO-ZnO and NiO-CuO nanocomposites for enhanced photocatalytic degradation of methylene blue under UV light irradiation. *Front Mater* **9**:832439 (2022). <https://doi.org/10.3389/fmats.2022.832439>.
- 38 Shim YJ, Soshnikova V, Anandapadmanaban G, Mathiyalagan R, Jimenez Perez ZE, Markus J et al., Zinc oxide nanoparticles synthesized by *Suaeda japonica* Makino and their photocatalytic degradation of methylene blue. *Optik (Stuttg)* **182**:1015–1020 (2019).
- 39 Suba S, Vijayakumar S, Vidhya E, Punitha VN and Nilavukkarasi M, Microbial mediated synthesis of ZnO nanoparticles derived from *Lactobacillus* spp: characterizations; antimicrobial and biocompatibility efficiencies. *Sens Int* **2**:100104 (2021).
- 40 Ekennia AC, Uduagwu DN, Nwaji NN, Oje OO, Emma-Uba CO, Mgbii SI et al., Green synthesis of biogenic zinc oxide nanoflower as dual agent for photodegradation of an organic dye and tyrosinase inhibitor. *J Inorg Organomet Polym Mater* **31**:886–897 (2021).
- 41 Haque S, Faidah H, Ashgar SS, Abujamel TS, Mokhtar JA, Almuhayawi MS et al., Green synthesis of Zn(OH)₂/ZnO-based bionanocomposite using pomegranate peels and its application in the degradation of bacterial biofilm. *Nanomaterials* **12**:3458 (2022). <https://doi.org/10.3390/nano12193458>.
- 42 Park JK, Rupa EJ, Arif MH, Li JF, Anandapadmanaban G, Kang JP et al., Synthesis of zinc oxide nanoparticles from *Gynostemma pentaphyllum* extracts and assessment of photocatalytic properties through malachite green dye decolorization under UV illumination: a green approach. *Optik (Stuttg)* **239**:166249 (2021).
- 43 Ramesh P, Rajendran A and Ashokkumar M, Biosynthesis of zinc oxide nanoparticles from *Phyllanthus niruri* plant extract for photocatalytic and antioxidant activities. *Int J Environ Anal Chem* (2022).
- 44 Dappula SS, Kandrakonda YR, Shaik JB, Mothukuru SL, Lebaka VR, Mannarapu M et al., Biosynthesis of zinc oxide nanoparticles using aqueous extract of *Andrographis alata*: characterization; optimization and assessment of their antibacterial; antioxidant; antidiabetic and anti-Alzheimer's properties. *J Mol Struct* **1273**:134264 (2023).
- 45 Stan M, Popa A, Toloman D, Silipas T-D and Vodnar DC, Antibacterial and antioxidant activities of ZnO nanoparticles synthesized using extracts of *Allium sativum*; *Rosmarinus officinalis* and *Ocimum basilicum*. *Acta Metallurgica Sinica (English Letters)* **29**:228–236 (2016).
- 46 AlSalhi MS, Devanesan S, Atif M, AlQahtani WS, Nicoletti M and Del Serrone P, Therapeutic potential assessment of green synthesized zinc oxide nanoparticles derived from fennel seeds extract. *Int J Nanomedicine* **15**:8045–8057 (2020).
- 47 Ifeanyichukwu UL, Fayemi OE and Ateba CN, Green synthesis of zinc oxide nanoparticles from pomegranate (*Punica granatum*) extracts and characterization of their antibacterial activity. *Molecules* **25**:4521 (2020).
- 48 Balogun FO and Ashafa AOT, Potentials of synthesised *Lessertia montana* zinc oxide nanoparticles on free radicals-mediated oxidative stress and carbohydrate-hydrolysing enzymes. *Acta Biologica Szegediensis* **64**:239–249 (2021).
- 49 Manasa DJ, Chandrashekar KR, Pavan Kumar MA, Suresh D, Madhu Kumar DJ, Ravikumar CR et al., Proficient synthesis of zinc oxide nanoparticles from *Tabernaemontana heyneana* Wall. via green combustion method: antioxidant; anti-inflammatory; antidiabetic; anticancer and photocatalytic activities. *Results Chem* **3**:100178 (2021).
- 50 Dar A, Rehman R, Zaheer W, Shafique U and Anwar J, Synthesis and characterization of ZnO-nanocomposites by utilizing aloe vera leaf gel and extract of *Terminalia arjuna* nuts and exploring their antibacterial potency. *J Chem* **2021**:9448894 (2021).
- 51 Yassin MT, Mostafa AA-F, Al-Askar AA and Al-Otibi FO, Facile green synthesis of zinc oxide nanoparticles with potential synergistic activity with common antifungal agents against multidrug-resistant candidal strains. *Crystals (Basel)* **12**:774 (2022). <https://doi.org/10.3390/cryst12060774>.
- 52 Venkatesan S, Suresh S, Ramu P, Kandasamy M, Arumugam J, Thambidurai S et al., Biosynthesis of zinc oxide nanoparticles using *Euphorbia milii* leaf constituents: characterization and improved photocatalytic degradation of methylene blue dye under natural sunlight. *J Indian Chem Soc* **99**:100436 (2022).
- 53 Ahmad M, Rehman W, Khan MM, Qureshi MT, Gul A, Haq S et al., Phyto-genic fabrication of ZnO and gold decorated ZnO nanoparticles for photocatalytic degradation of Rhodamine B. *J Environ Chem Eng* **9**:104725 (2021).
- 54 Zewde D and Geremew B, Biosynthesis of ZnO nanoparticles using *Hagenia abyssinica* leaf extracts; their photocatalytic and antibacterial activities. *Environ Pollut Bioavailab* **34**:224–235 (2022).
- 55 Yashni G, Al-Gheethi A, Radin Mohamed RMS, Dai-Viet NV, Al-Kahtani AA, Al-Sahari M et al., Bio-inspired ZnO NPs synthesized from *Citrus sinensis* peels extract for Congo red removal from textile wastewater via photocatalysis: optimization; mechanisms; techno-economic analysis. *Chemosphere* **281**:130661 (2021).
- 56 López-Agama I, Ramos-García MDL, Zamilpa A, Bautista-Baños S and Ventura-Aguilar RI, Comparative analysis of the antioxidant compounds of raw edible flowers and ethanolic extracts of *Cucurbita pepo*; *Tagetes erecta*; and *Erythrina americana* during storage. *J Food Process Preserv* **45**:e15842 (2021).
- 57 Elhusseiny SM, El-Mahdy TS, Awad MF, Elleboudy NS, Farag MMS, Yassein MA et al., Proteome analysis and in vitro antiviral; anticancer and antioxidant capacities of the aqueous extracts of *Lentinula edodes* and *Pleurotus ostreatus* edible mushrooms. *Molecules* **26**:4623 (2021). <https://doi.org/10.3390/molecules26154623>.
- 58 Ameen F, Dawoud T and AlNadhari S, Ecofriendly and low-cost synthesis of ZnO nanoparticles from *Acremonium potronii* for the photocatalytic degradation of azo dyes. *Environ Res* **202**:111700 (2021).
- 59 Chen L, Batjikh I, Hurh J, Han Y, Huo Y, Ali H et al., Green synthesis of zinc oxide nanoparticles from root extract of *Scutellaria baicalensis* and its photocatalytic degradation activity using methylene blue. *Optik (Stuttg)* **184**:324–329 (2019).
- 60 Lu J, Ali H, Hurh J, Han Y, Batjikh I, Rupa EJ et al., The assessment of photocatalytic activity of zinc oxide nanoparticles from the roots of *Codonopsis lanceolata* synthesized by one-pot green synthesis method. *Optik (Stuttg)* **184**:82–89 (2019).
- 61 Sadiq H, Sher F, Sehar S, Lima EC, Zhang S, Iqbal HMN et al., Green synthesis of ZnO nanoparticles from *Syzygium cumini* leaves extract with robust photocatalysis applications. *J Mol Liq* **335**:116567 (2021).
- 62 Shubha JP, Kavalli K, Adil SF, Assal ME, Hatshan MR and Dubasi N, Facile green synthesis of semiconductive ZnO nanoparticles for photocatalytic degradation of dyes from the textile industry: a kinetic approach. *J King Saud Univ Sci* **34**:102047 (2022).
- 63 Mekonnen G, Negash A, Gashu M and Tadesse NB, *Echinops kebericho* aqueous root extract assisted green synthesis of zinc oxide nanoparticles for photocatalytic degradation of methylene blue. *Lett Appl NanoBioScience* **12**:72 (2023).
- 64 Saad Algarni T, Abdul NA, Al Kahtani A and Aouissi A, Photocatalytic degradation of some dyes under solar light irradiation using ZnO nanoparticles synthesized from *Rosmarinus officinalis* extract. *Green Chem Lett Rev* **15**:460–473 (2022).
- 65 Sai Saraswathi V, Tatsugi J, Shin PK and Santhakumar K, Facile biosynthesis, characterization, and solar assisted photocatalytic effect of ZnO nanoparticles mediated by leaves of *L. speciosa*. *J Photochem Photobiol B* **167**:89–98 (2017).
- 66 Sayadi MH, Ghollasimood S, Ahmadpour N and Homaeigohar S, Biosynthesis of the ZnO/SnO₂ nanoparticles and characterization of their photocatalytic potential for removal of organic water pollutants. *J Photochem Photobiol A* **425**:113662 (2022).
- 67 Shahinyan GA, Amirbekyan AY and Markarian SA, Photophysical properties of methylene blue in water and in aqueous solutions of dimethylsulfoxide. *Spectrochim Acta A* **217**:170–175 (2019).
- 68 Li FT, Zhao Y, Liu Y, Hao YJ, Liu RH and Zhao DS, Solution combustion synthesis and visible light-induced photocatalytic activity of mixed amorphous and crystalline MgAl₂O₄ nanopowders. *Chem Eng J* **173**:750–759 (2011).
- 69 Phonsy P, Anju SG, Jyothi K, Yesodharan S and Yesodharan E, Semiconductor mediated photocatalytic degradation of plastics and recalcitrant organic pollutants in water: effect of additives and fate of in situ formed H₂O₂. *J Adv Oxid Technol* **18**:85–97 (2015). <https://doi.org/10.1515/jaots-2015-0111>.
- 70 Hou H, Zeng X and Zhang X, Production of hydrogen peroxide by photocatalytic processes. *Angew Chem Int Ed* **59**:17356–17376 (2020).
- 71 Mahana A and Mehta SK, Potential of *Scenedesmus*-fabricated ZnO nanorods in photocatalytic reduction of methylene blue under direct sunlight: kinetics and mechanism. *Environ Sci Pollut Res* **28**:28234–28250 (2021).
- 72 Khan I, Saeed K, Zekker I, Zhang B, Hendi AH, Ahmad A et al., Review on methylene blue: its properties, uses, toxicity and photodegradation. *Water (Basel)* **14**:242 (2022). <https://doi.org/10.3390/w14020242>.